Nanolayered Material – Coating Prototypes

ET-0005B-14

I. M. Pinto and the Uni Sannio ELiTES Team

on behalf of ELiTES WP2

Nanolayered Film Prototypes for Optical Coatings

I.M. Pinto on behalf of the UniSannio ELiTES Working Group

1.1 Introduction and Rationale

By nanolayered films we mean a stack of alternating planar high/low index glassy oxide layers whose thicknesses are much smaller than the optical (and acoustical) wavelength(s) of interest. These films can be treated as effectively *homogeneous* media, and their optical (complex refractive index) and viscoelastic (complex Young modulus) properties can be computed using effective-medium approaches, as summarized below.

Nanolayered glassy films could be an interesting alternative to co-sputtered glassy mixtures (Pinto et al., 2011). These latter, whose best known and most successful paradigm is the TiO_2 doped Ta_2O_5 formula developed at LMA (Harry et al., 2007) represent to date the most successful attempt toward reducing coating thermal noise by *engineering* the coating materials.

We designed several nanolayered-films consisting of alternate sub-layers of SiO_2 and TiO_2, all having the same (effective, macroscopic) nominal refractive index and optical thickness, but differing in the number and thickness of the nanolayers.

Prototypes of these films designed by the ELiTES UniSannio Team were manufactured by and characterized, as regards their morphological and mechanical (loss angle) properties in collaboration with prof. S. Chao and co-Workers at the National Tsing Hua University in Taiwan (ROC).

Titania (TiO_2) has the largest refractive index (2.33 at $1064nm$) among all glassy oxides currently in use for high quality optical coatings, and a relatively low mechanical loss angle when in the amorphous state (Scott and MacCrone, 1968). A large index (or more precisely, a large contrast between the low and high index coating constituents) is beneficial to reduce the number of doublets needed to achieve a specificied reflectance, and hence, potentially, the coating noise. Unfortunately (similar to Hafnia) Titania films thicker than a few nm crystallize after annealing, (Sankur and Gunning (1989), Gluck et al. (1991), Wang and Chao (1998), Chao et al. (1999), Chao et al. (2001)), with subsequent blow up of mechanical and optical losses (Amico et al., 2006). This prevented so far the use of Titania (and Hafnia) for building high reflectance, low loss and low noise coatings.

Silica (SiO_2), on the other hand, is the most stable (and less lossy) glassy oxide available.

Experience in nanolayered film technology from X-ray mirror research (F. Erickson et al (2006), E. Maykova et al. (2006)) suggests that by progressively reducing the thickness of the alternating nanolayers (while keeping the effective optical index and thickness of the whole nanolayered film unchanged) we should be able to prevent the formation and subsequent growth during the annealing phase of TiO_2 crystallites (crystal nucleation centers), hopefyully resulting into an amorphous composite material with nicely large refractive index, and fairly low optical and mechanical losses. This would allow the use of glassy oxides like Titania and Hafnia which do not exhibit a sensible peak in their mechanical losses at cryo temperaturs, and are thus interesting for cryogenic interferometers like KAGRA and ET.

1.2 Nanolayered Film Modeling

Effective medium theory (EMT) provides a natural framework for modeling the optical and mechanical (viscoelastic) properties of nanolayered composites. We shall limit here to the simplest case where diffusion at the interfaces can be neglected. EMT can be used to handle this latter, in principle, at the expense of extra formal complications.

1.2.1 Refractive Index of Nanolayered Film

The effective complex refractive index of the nanolayered film is given by the following formula credited to Drude :

$$n_f = \left[r_H n_H^2 + (1 - r_H) n_L^2\right]^{1/2} \tag{1.1}$$

where r_h is the thickness (and volume) fraction of the high index constituent.

1.2.2 Young Modulus of Nanolayered Film

The Young modulus of a plane layered stack of isotropic homogeneous materials takes two different forms. Letting $Y_{H,L}$ the bulk Young moduli of the constituents, for parallel stresses, the effective Young modulus is given by Voigt formula:

$$Y_f^{||} = r_H Y_H + (1 - r_H) Y_L; \tag{1.2}$$

for perpendicular stresses, it is given by Reuss formula:

$$Y_f^{\perp} = [r_H / Y_H + (1 - r_H)/Y_L]^{-1} \tag{1.3}$$

The formula to use to compute the energy ratio of a clamped cantilever oscillator in the lowest flexural mode, where stresses are predominantly parallel is Voigt's; the formula to use for coating loss-angle characterization, which follows from applying a time-harmonic driving force normal to the coating face and using the Fluctuation-Dissipation Theorem, is that of Reuss.

1.2.3 Loss Angle of Nanolayered Film

Following (Harry et al., 2012) the mechanical loss angle of a multilayer film-coating, consisting of (alternating) high and low index materials, in the limit of vanishingly small Poisson ratios, can be written

$$\phi_c = \pi^{-1/2} w^{-1} \left[\left(\frac{Y_s}{Y_H} + \frac{Y_H}{Y_s} \right) z_H \phi_H + \left(\frac{Y_s}{Y_L} + \frac{Y_L}{Y_s} \right) z_L \phi_L \right] \tag{1.4}$$

where $z_{L,H}$ is the total *metric* thickness of the high/low index layers, Y_s is the Young modulus of the substrate, and w is the laser beam width. For a nanolayered coating

$$z_H = r_H h_f, \; z_L = (1 - r_H) h_f \tag{1.5}$$

where h_f is the total thickness of the film, and r_H is the thickness (volume) fraction of the high index material. The formula obtained letting (1.5) in (1.4) should be compared to equation (1.4) written for an equivalent *homogeneous* layer with thickness h_f, loss angle ϕ_f and Young modulus Y_f,

$$\phi_c = \pi^{-1/2} w^{-1} \left(\frac{Y_s}{Y_f} + \frac{Y_f}{Y_s} \right) \phi_f h_f \tag{1.6}$$

yielding

$$\phi_f = \frac{\left(\frac{Y_s}{Y_H} + \frac{Y_H}{Y_s} \right) r_H \phi_H + \left(\frac{Y_s}{Y_L} + \frac{Y_L}{Y_s} \right) (1 - r_H) \phi_L}{Y_s \left[r_H / Y_H + (1 - r_H)/Y_L \right] + Y_s^{-1} \left[r_H / Y_H + (1 - r_H)/Y_L \right]^{-1}} \tag{1.7}$$

where Reuss formula (1.3) has been used to evaluate Y_f. Note that for $r_H = 1$ (resp., $r_H = 0$) i.e., for homogeneous nanolayers made of high (resp., low) index material, eq. (1.7) returns ϕ_H (resp., ϕ_L), as expected.

1.3 Nanolayered Film Prototypes

A number of SiO_2/TiO_2 nanolayered prototypes featuring *the same* nominal r_H, and hence the same (nominal) effective refractive index and Young modulus, all having the same nominal metric and optical thickness were manufactured using an ad hoc ion assisted magnetron sputtering coating deposition facility described in detail in (Chao et al., 2011) and shown in Figure 1 (top panel). The prototypes' geometry is summarized in Figure 2.

1.3.1 Morphology before Annealing

The microstructural morphology of the nanolayered prototypes before annealing was investigated using tunnel electron microscopy (TEM) and X-ray diffraction patterns (XRD). Illustrative results are shown in Figure 3. TEM images show no evidence of interfacial diffusion, and the deposition appears very clean and uniform down to thicknesses of a few nm. Systematic errors of a few percent in the deposition rate are noted, but these can be corrected, and do not ultimately affect the main results of the analysis. X ray diffraction patterns, on the other hand, show no evidence of crystal growth, even though tiny nucleation centers will most certainly be present, as in any sputter-deposited coating.

1.3.2 Film Loss Angle

The mechanical loss angle of the nanolayered films was measured prior to annealing using a clamped-cantilever setup described in (Chao et al., 2011)) .
We expected the nanolayered film loss angles to decrease by increasing the number of nanolayers, in view of the fact that the TiO_2 loss angle should decrease with the expected reduction in the number and size of the nucleation centers

(Chao et al., 2001).
The loss angle was measured for the first (fundamental) flexural cantilever eigenmode before and after depositing the nanolayered film on the bare cantilevers, using the following formula to retrieve the loss angle of the nanolayered film from the two measurements (see (Pierro and Pinto, 2006) and (Comtet et al., 2007)).

$$\phi_f = \eta_E \left(\phi_{coated} - \phi_{bare}\right) \tag{1.8}$$

where (Pierro and Pinto, 2006), (Comtet et al., 2007)

$$\eta_E = \frac{Y_s h_s}{3Y_f^{||} h_f} = \frac{Y_s h_s}{3Y_f^{||}(z_L + z_H)} \tag{1.9}$$

is the ratio between the eigenmode energies in the substrate and the nanolayered film, Y_s, h_s and Y_f, h_f being the Young modulus and (metric) thickness of the naked substrate and nanolayered film, respectively.
Some results are shown in Figure 4. Preliminary measurements indicate that the film loss angle becomes smaller after decreasing the thickness of the TiO_2 nanolayers, according to our predictions.

1.3.3 Titania Loss Angles before Annealing

The loss angle measurements made on a cantilever coated with a single-layer of SiO_2 can be used to retrieve the loss angle ϕ_L of un-annealed Silica. A value for this latter of $4.06 \cdot 10^{-4}$ was obtained, and assumed to be the same, independent from the thickness of the Silica layers, for all prototypes.
This value of ϕ_L can be used in turn, via eq. (1.7), to retrieve the loss angle of TiO_2, as a function of thickness of the TiO_2 layers, from the measured loss angles of films with a different number of nanolayers.
The result is illustrated in Figure 5. As the the Titania nanolayers' thickness drops from $13.7nm$ (11-layers prototype) to $7.36nm$ (19-layers prototype), the estimated retrieved mechanical loss angle of un-annealed Titania drops from $\approx 1.3 \cdot 10^{-3}$ to $\approx 5.9 \cdot 10^{-4}$. This is comparable to the loss angle of un-annealed Titania doped Tantala (see, e.g., fig. 4 in (Comtet et al., 2007)).

1.3.4 Error Propagation

Error bars on all measured quantities were computed using standard error propagation formulas. Accordingly, given a quantity $y = f(x_1, x_2, \ldots, x_n)$ where $f(\cdot)$ is a smooth (differentiable) function of its arguments, the expected value and the std. deviation of y are computed as

$$\begin{cases} \langle y \rangle = f(\langle x_1 \rangle, \langle x_2 \rangle, \ldots, \langle x_n \rangle) \\ \sigma_y = \langle (y - \langle y \rangle)^2 \rangle^{1/2} = \left[\sum_{i=1}^{n} \left(\frac{\partial f}{\partial x_i} \right)^2 \sigma_{x_i}^2 \right]^{1/2} \end{cases} \tag{1.10}$$

where the x_i are fiducially assumed as being Gaussian distributed and statistically independent (Clifford, 1973). In our specific case, it is reasonable to treat the susbstrate and layer thicknesses, and the material properties (refractive index and Young modulus) as independent quantities, with known average values and std. deviations, and compute the expected values and std.deviations of all quantities of interest using eqs. (1.10).
To do so, we note that *all* quantities of interest , i.e., eqs. (1.1), (1.2), (1.3), (1.7), (1.8) and (1.9) depend on the layer thicknesses $z_{L,H}^{(i)}$ *only* through the quantities

$$z_{L,H} = \sum_i z_{L,H}^{(i)}, \tag{1.11}$$

whose averages and std. deviations are

$$\langle z_{L,H} \rangle = \sum_i \langle z_{L,H}^{(i)} \rangle, \quad \sigma_{z_{L,H}} = \left[\sum_i \left(\sigma_{z_{L,H}^{(i)}} \right)^2 \right]^{1/2}. \tag{1.12}$$

1.3.5 Morphology after Annealing

A subset of the nanolayered prototypes has been subsequently annealed, for different annealing times, and their morphology investigated by SEM, AFM and X-ray diffraction.
The results are illustrated in Figures 6 to 8.
Crystalline transition is observed in the Titania nanolayers at increasing temperatures (and baking times) as their thickness is reduced. This is clearly shown by the X-ray diffraction patterns in Figure 6, where for a fixed annealng time and temperature, the Anatase line signaling crystallization becomes broader and less tall as thickness is reduced, witnessing increased crystal growth frustration, until it disappears completely.
Prelimary estimates of the crystallite size as a function of the nanolayer thickness, based on Scherrer's model (Klug and Leroy, 1974) indicate that average crystallite size scales lineraly with (and does not exceed) the nanolayer thickness (Chao et al., 2013), in agreement with early findings in (Sankur and Gunning, 1989). This seems to be pictorially confirmed by the AFM pictures in Figure 8. Measurement of the transverse (in-layer) crystallite size via modified AFM is in progress.

1.3.6 Loss Angle after Annealing

Loss angle measurements on annealed nanolayered prototypes were under way at the moment of this writing.
The whole cantilever based measurement setup at NTHU has meanwhile undergone a substantial redesign, following the observation of poor measurement repeatability due to cantilever surface degradation produced by the clamping vise, also in preparation of cryogenic measurements.

1.4 Conclusions

Preliminary results on nanolayered SiO_2/TiO_2 film prototypes with different number and thicknesses of the nanolayers, all having the same nominal optical index and thickness ($n = 2.09$, $d =$ one quarter of wavelength at $1064nm$) indicate that crystallite formation is reduced by reducing the TiO_2 nanolayer thickness, and that crystallite growth upon annealing is effectively frustrated end eventually suppressed by thinning the nanolayers. Loss angle measurements on the annealed prototypes will be available soon. A successful outcome of this research program may open the road to an interesting new class of cryogenic (and room temperature) dielectric mirror materials.

Acknowledgements

This work has been carried out in collaboration with the group led by Professor Shiuh Chao at the Tsing-Hua National University of Taywan, ROC (S. Chao, J.-S. Ou, Y.-H. Juang, V. Huang, L.-C. Kuo, S.-J. Song, S.-J. Wang, S. Wang, H. Pan, C.-W. Lee), and has been supported in part by the the National Science Council of Taiwan, under the NSC-100-2221-E-007-099-MY3 project grant, by the National Tsing Hua University under the 101N2501E1 project grant, and by the Italian National Institute for Nuclear Physics (INFN) under the CSN-V MIDI-BRUT grant.

Bibliography

P. Amico et al., "Investigation on mechanical losses in TiO_2/SiO_2 Dielectric Coatings," J. Phys. Conf. Ser. 32 (2006) 413.

S. Chao et al., "Characteristics of Ion-Beam-Sputtered High-Refractive-Index TiO2-SiO2 Mixed Films," J. Opt. Soc. Am., **A16** (1999) 1477.

S. Chao et al., "Low-Loss Dielectric Mirror with Ion-Beam-Sputtered TiO_2 SiO_2 Mixed Films," Applied Opt., **40** (2001) 2177.

S. Chao et al., "Progress update on coating preparation at NTHU," LIGO/G1101083 (2011).

S. Chao et al., "Progress of Coating Development at NTHU," LIGO/G1200849 (2012).

S. Chao et al., "Thickness-Dependent Crystallization on Thermal Anneal for the Titania/Silica Nano-Layers Deposited by Ion-Beam-Sputter Method," LIGO-G1300921 (2013).

A.A. Clifford, *Multivariate Error Analysis: a Handbook of Error Propagation and Calculation in Many Parameter Systems,* J. Wiley & Sons, New York, (1973).

Ch.Comtet et al., "Reduction of Tantala Mechanical Losses in Ta_2O_5/SiO_2 Coatings for the Next Generation of Virgo and LIGO Interferometric Gravitational Wave Detectors, " 42th Rencontres de Moriond - Gravitational Waves and Experimental Gravity, La Thuile, IT (2007), HAL: in2p3-00177578.

F. Erickson et al., "Interface Engineering of Short-Period Ni/V Multilayer X-ray Mirrors," Thin Solid Films **500** (2006) 84.

N.S. Gluck et al., "Microstructure and Composition of Composite SiO2/TiO2 Thin Films," J. Appl. Phys. **69** (1991) 3037.

G. Harry et al., "Titania-doped tantala/silica coatings for gravitational-wave detection," Class. Quantum Grav. bf 24 (2007) 405.

I.M. Pinto et al., "Reflectivity and Thickness Optimization," Chapter 12 in G. Harry et al., *Optical Coatings in Precision Measurements*, Cambridge University Press (2012).

H.P. Klug and A.E. Leroy "*X-Ray Diffraction Procedures for Polycrystalline and Amorphous Materials*,"J. Wiley & Sons, New York (1974).

M. Maykova et al., "Nanometer-scale period Sc/Cr multilayer mirrors and their thermal stability," Thin Solid Films **497** (2006) 115.

V.Pierro and I.M. Pinto, "Measuring Coating Mechanical Quality Factors in a Layered Cantilever Geometry: a Fully Analytic Model," LIGO Document T060173 (2006)

I.M. Pinto et al., "Subwavelength Layered Titania-Silica for Advanced Interferometer Coatings," LIGO-G1100586 (2011).

H.Q. Sankur and W.J. Gunning, "Crystallization and Diffusion in Composite TiO2-SiO2 Thin Films," J.Appl. Phys., **66** (1989) 4747.

W.W. Scott and R.K. MacCrone, "Apparatus for Mechanical Loss Measurements at Audio Frequencies and Low Temperatures," Rev. Sci. Instr. **39** (1968) 821.

W.H. Wang and S. Chao, "Annealing Effect on Ion-Beam-Sputtered Titanium Dioxide Film," Optics Lett., **23** (1998) 1417.

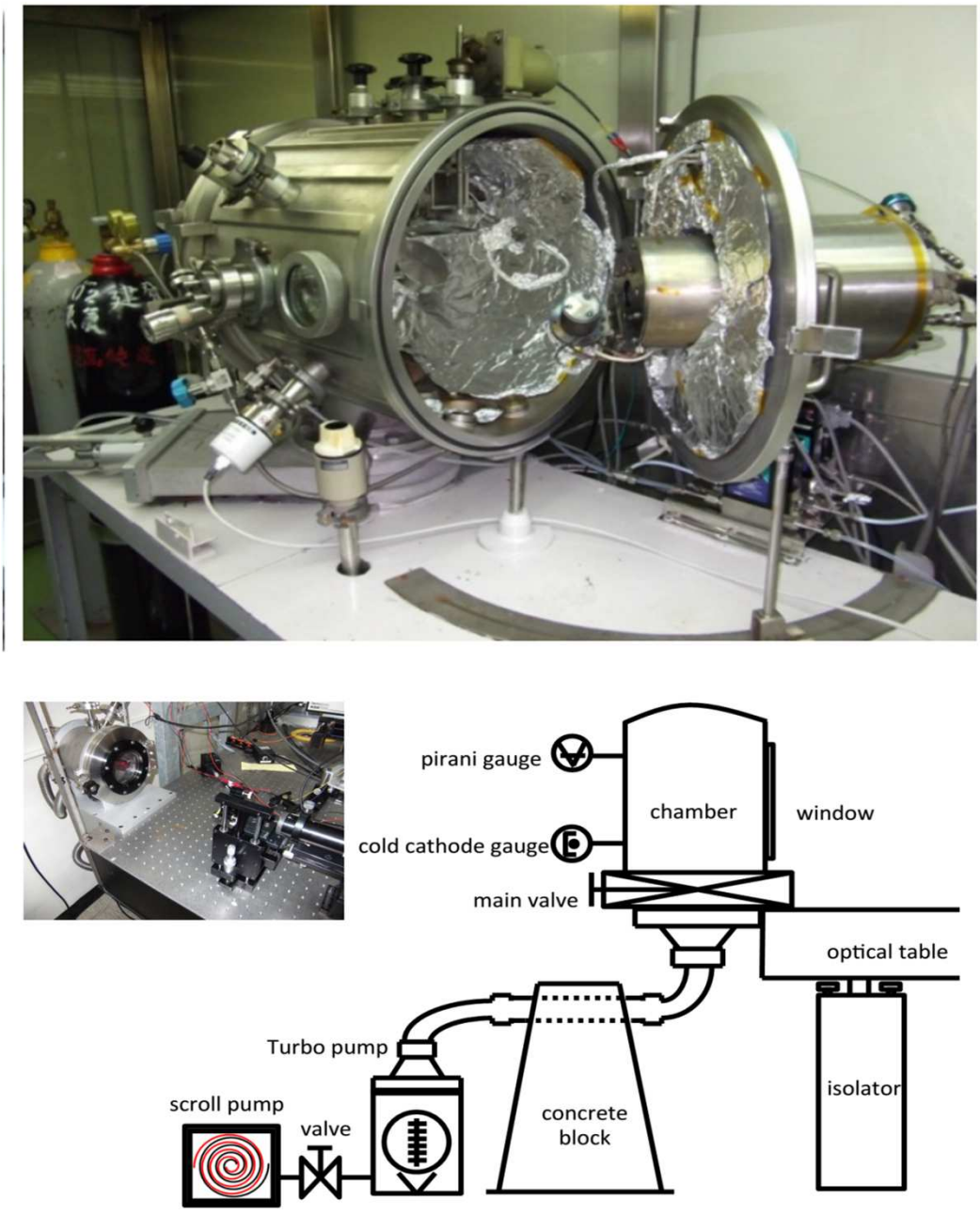

Figure 1 – Coating facility (top) and cantilever-based loss angle measurement facility (bottom) at NTHU.

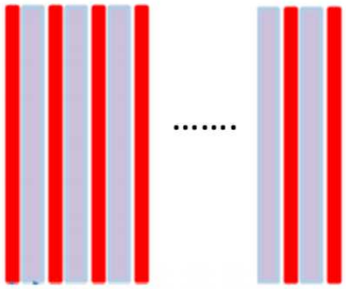

N TiO2	Thickness TiO2 [nm]	N SiO2	Thickness SiO2
2	42.56	1	42.15
3	28.37	2	21.07
4	21.28	3	14.05
5	17.02	4	10.54
6	14.19	5	8.43
7	12.16	6	7.02
8	10.64	7	6.02
9	9.46	8	5.27
10	8.51	9	4.68

Figure 2 – Some nanolayered prototypes designed by the UniSannio ELiTES Working Group. All prototypes have n = 2.09, nominal physical thickness of 127.3 nm, nominal optical thickness of 266 nm (one quarter of $\lambda = 1064$nm).

11 layer

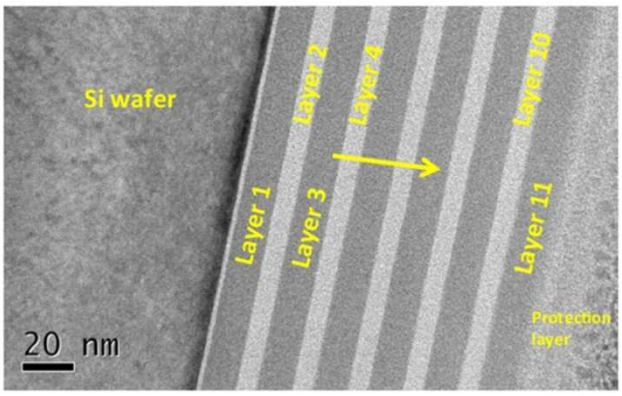

TiO_2		SiO_2	
Design thickness(nm)	14.19	Design thickness(nm)	8.41
Thickness ratio (TiO_2:SiO_2)= 1.69 : 1			
Layer	Measured thickness(nm)	Layer	Measured thickness(nm)
11	13.6±0.1	10	7.6±0.1
9	13.3±0.1	8	7.5±0.1
7	13.6±0.1	6	7.7±0.2
5	13.8±0.1	4	7.0±0.2
3	14.4±0.3	2	7.4±0.2
1	13.4±0.3		
Average	13.68	Average	7.44
Thickness ratio (TiO_2:SiO_2)= 1.84 : 1			
Total	119.3±1.1		

19 layer

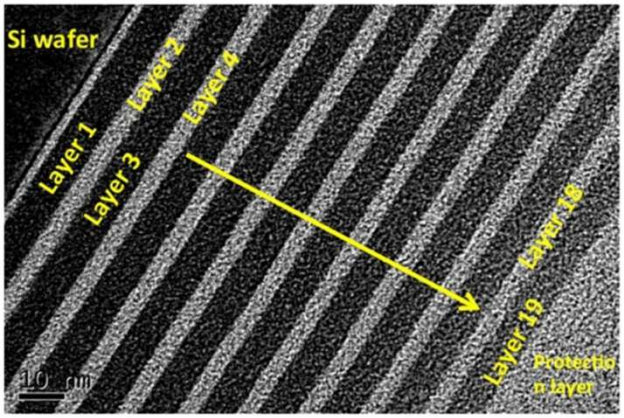

TiO_2		SiO_2	
Design thickness(nm)	8.51	Design thickness(nm)	4.68
Thickness ratio (TiO_2:SiO_2)= 1.82 : 1			
Layer	Measured thickness(nm)	Layer	Measured thickness(nm)
19	7.0±0.5	18	4.0±0.3
17	7.7±0.2	16	4.3±0.3
15	7.1±0.1	14	4.7±0.4
13	7.1±0.1	12	4.2±0.1
11	7.0±0.2	10	4.1±0.2
9	7.2±0.3	8	4.5±0.3
7	7.3±0.3	6	4.5±0.3
5	7.5±0.3	4	4.4±0.5
3	7.6±0.4	2	4.2±0.2
1	8.1±0.1		
Average	7.36	Average	4.32
Thickness ratio (TiO_2:SiO_2)= 1.70 : 1			
Total	112.6±1.2		

Figure 3 – TEM and XRD pictures of two nanolayered prototypes made at NTHU, before annealing.

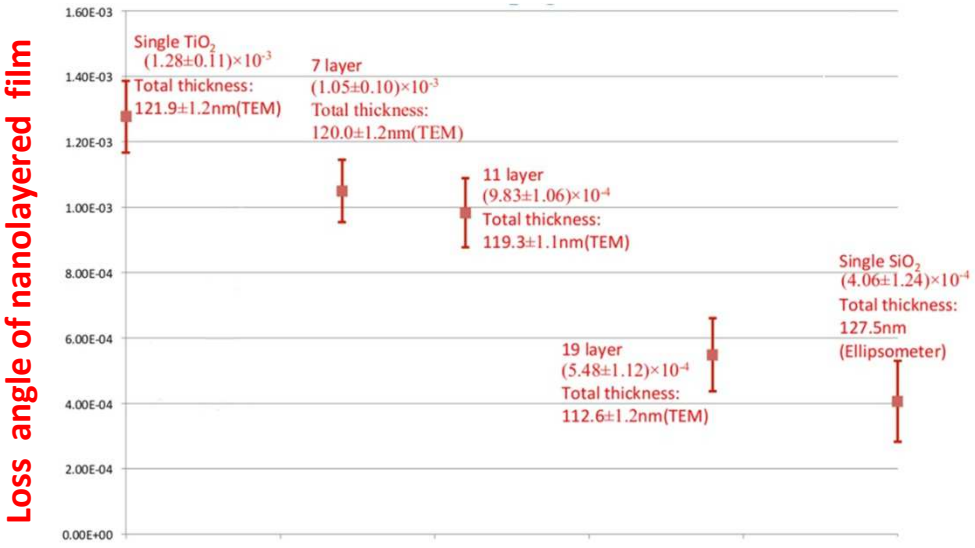

Figure 4 – Loss angle measured at NTHU of some nano-layered prototypes before annealing.

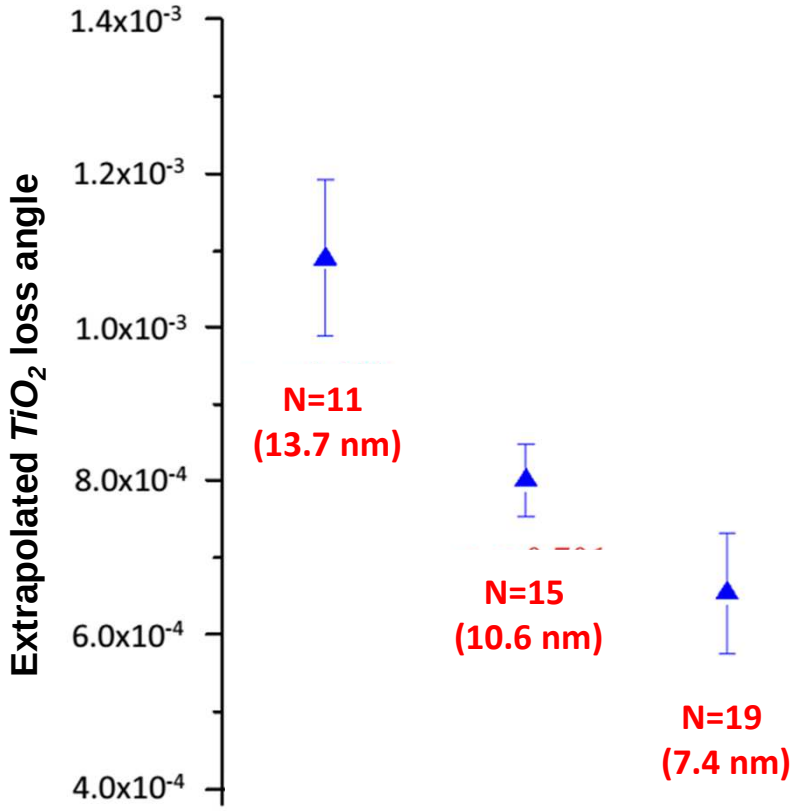

Figure 5 – Extrapolated TiO_2 mechanical loss angle for three nanolayered prototypes with different number and thickness of the nanolayers.

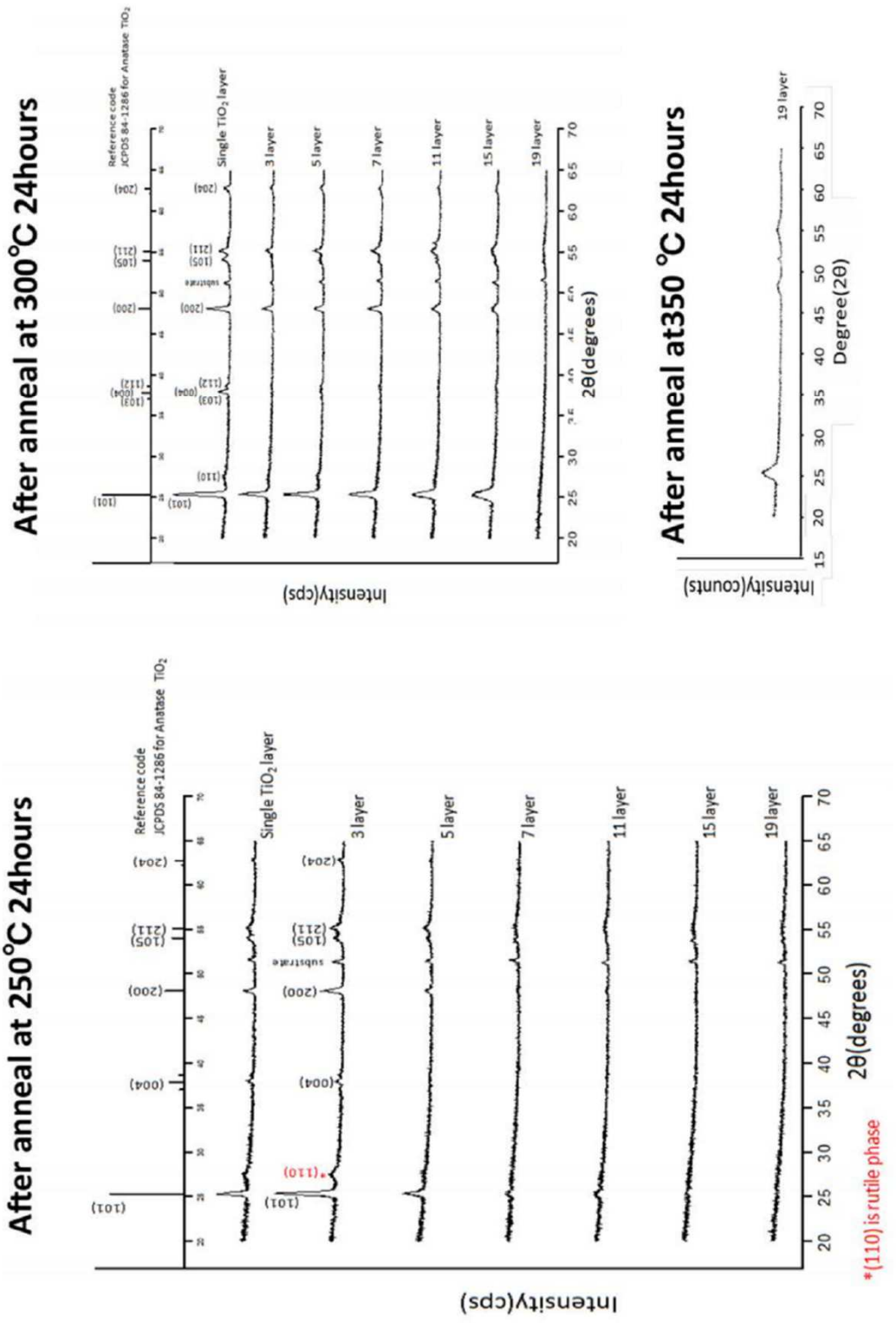

Figure 6 – XRD spectra of nanolayered prototypes made at NTHU after annealing (24h) at different temperatures.

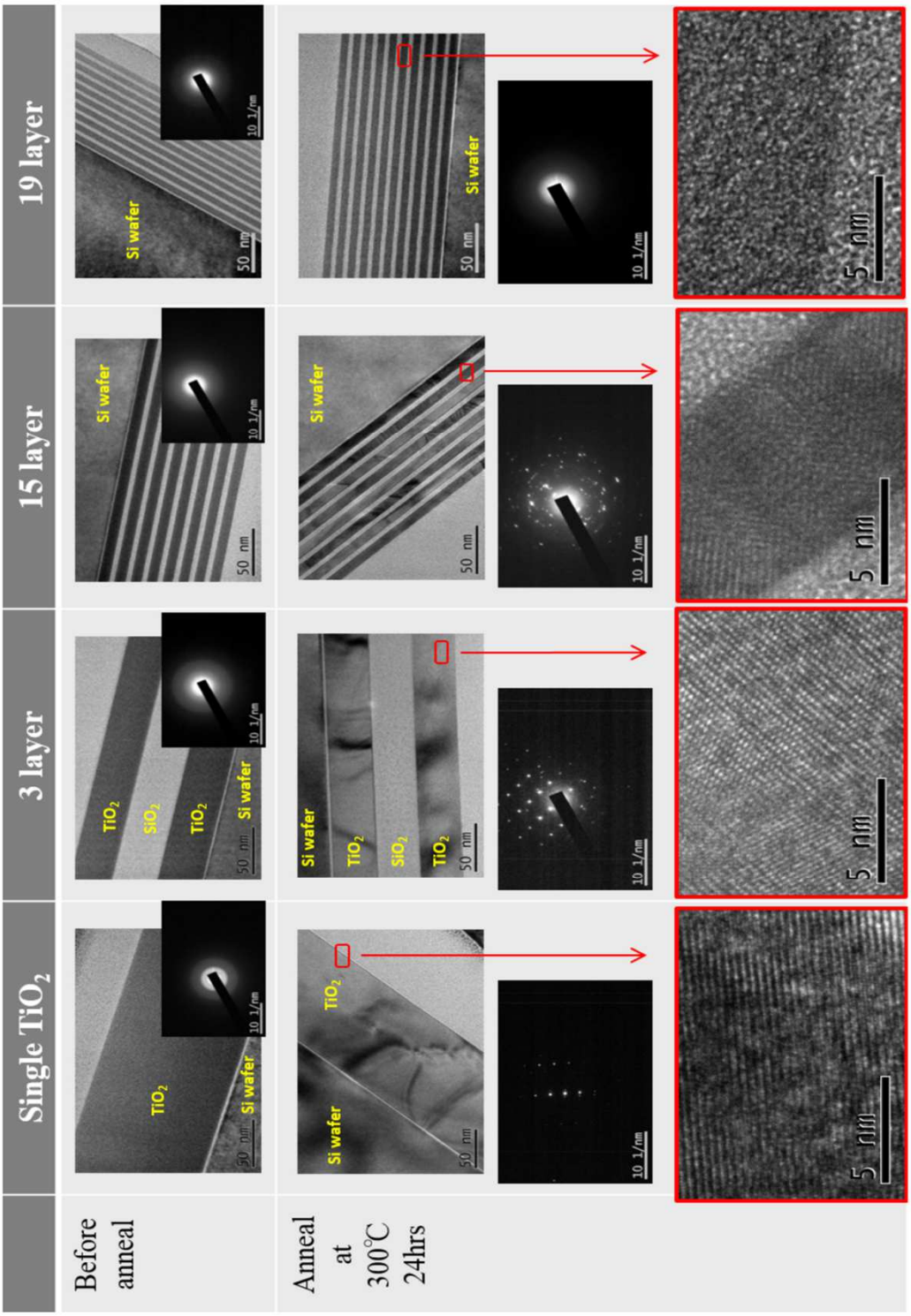

Figure 7 – TEM images of nanolayered prototypes made at NTHU before and after annealing (24h at 300C) .

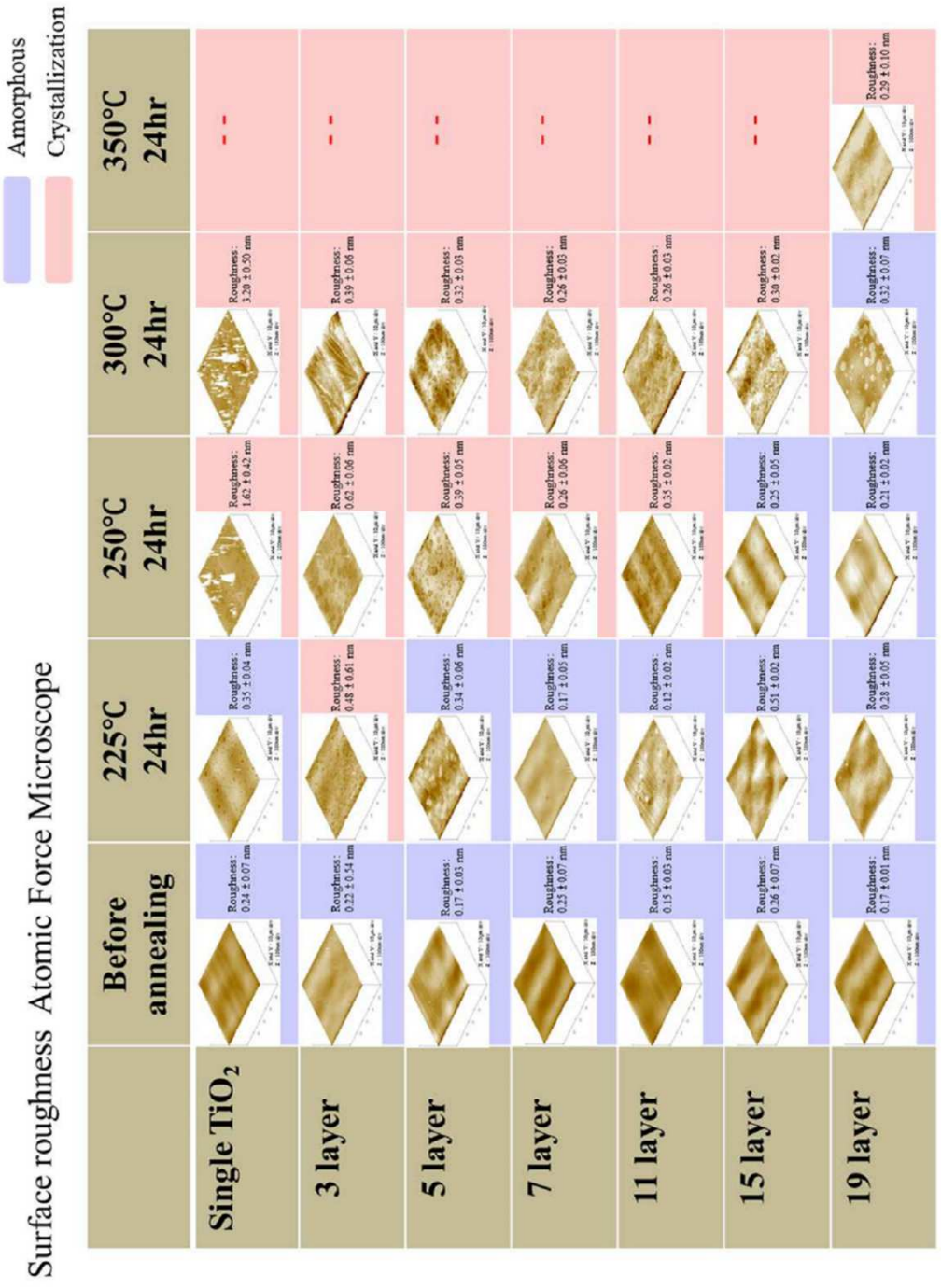

Figure 8 – AFM imaging of nanolayered prototypes made at NTHU after anealing (24h) at different temperatures.